Proc. 3rd Intern. EuroConf. on Advanced Semiconductor Devices and Microsystems - ASDAM 2000, 16-18 Oct 2000, Smolenice Castle, Slovakia (2000) 251-254

Homogeneity of InGaAs/InP Nanostructures

D. Piester, A. A. Ivanov, A. S. Bakin, T. Klaffs, M. Ursu, H.-H. Wehmann, A. Schlachetzki, and S. Kipp[a]

Institut für Halbleitertechnik, Technische Universität Carolo-Wilhelmina, Hans-Sommer-Str. 66, D-38106 Braunschweig, Germany
e-mail: iht@tu-bs.de
[a]Institut für Physikalische und Theoretische Chemie, Technische Universität Carolo-Wilhelmina, Hans-Sommer-Str. 10, D-38106 Braunschweig, Germany

Atomic-force microscopy is applied to wet-chemically etched cleaved facets of InGaAs/InP nanoheterostructures. This technique allows the precise determination of process parameters relevant to advanced quantum devices realized by metal-organic vapor-phase epitaxy (MOVPE). We present data on thickness homogeneity and growth rates. We give evidence for the high quality of InGaAs/InP nanostructures grown by MOVPE.

1. Introduction

Atomic-force microscopy (AFM) is a standard method to investigate surfaces down to atomic resolution. However, only relatively few investigations were done on cross-sections of semiconductor heterostructures [1-4]. Yet in this field AFM has the potential to determine epitaxial layers in their thickness quickly and in a relatively simple way. As specific examples, advanced quantum devices, such as resonant-tunneling diodes [5] or quantum cascade lasers [6], fabricated by metal-organic vapor-phase epitaxy (MOVPE) rely on an efficient control of material parameters. In the present work we describe a method to determine the thickness homogeneity of epitaxially grown heterostructures and give evidence for the high quality of InGaAs/InP nanostructures grown by MOVPE. Furthermore the growth rates can be determined very precisely by this method. This is indispensable because “in situ“-systems like reflection high energy electron diffraction used during molecular-beam epitaxy are presently not avialable for MOVPE growth.

2. Sample Preparation

InP substrates (10×12 mm^2) with $(100) \pm 0.5°$ orientation and polished-surface finish were cleaned and loaded in a MOVPE-reactor designed by AIXTRON with an infrared-heated horizontal susceptor. As sources, we used trimethylindium and trimethylgallium as group-III precursors and arsine and phosphine as group-V precursors, respectively. The growth was performed at 640 °C and low pressure (20 hPa). The samples consist of an InP buffer on which six sequences, each made up of five nominally identical double-layers, were grown. A double-layer comprises an InP layer and an InGaAs, layer lattice-matched to InP. The structures were capped by InP. Two samples with different sequences were grown. For the first sample the ternary InGaAs growth duration t_t was varied from 16 to 96 s corresponding to a nominal thickness of about 10 to 61 nm, while the binary InP growth duration t_b remained constant (70 s, nominally 20 nm). The structure of Sample 1 is shown in Fig. 1. Sample 2

consists of sequences where t_t remained constant at 32 s (nominally 20 nm) while t_b was varied from 36 to 216 s. This is equivalent to nominal thickness of about 10 to 60 nm.

To prepare the samples for AFM measurements, they were cleaved along a {110} plane whose cross-sections were subsequently treated by selective wet-chemical etching of the InGaAs (see upper right corner of Fig. 1). This was done by applying the solution citric acid/H_2O_2 (7:1) for 5 s, yielding a surface corrugation which is easily accessible to AFM [2, 7].

3. Measurement Technique

The samples prepared as described above were studied in air by an AFM, model Discoverer TMX 2010 by TopoMetrix, in the contact mode. Commercial Si_3N_4 pyramidal

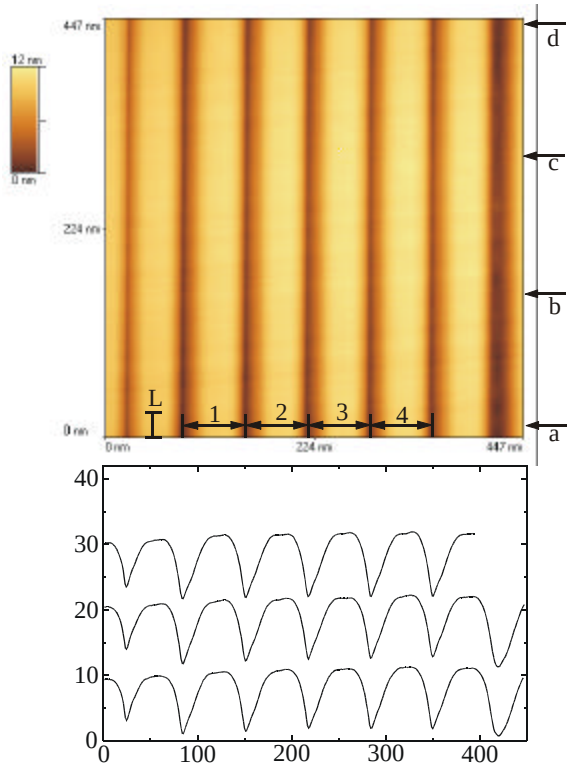

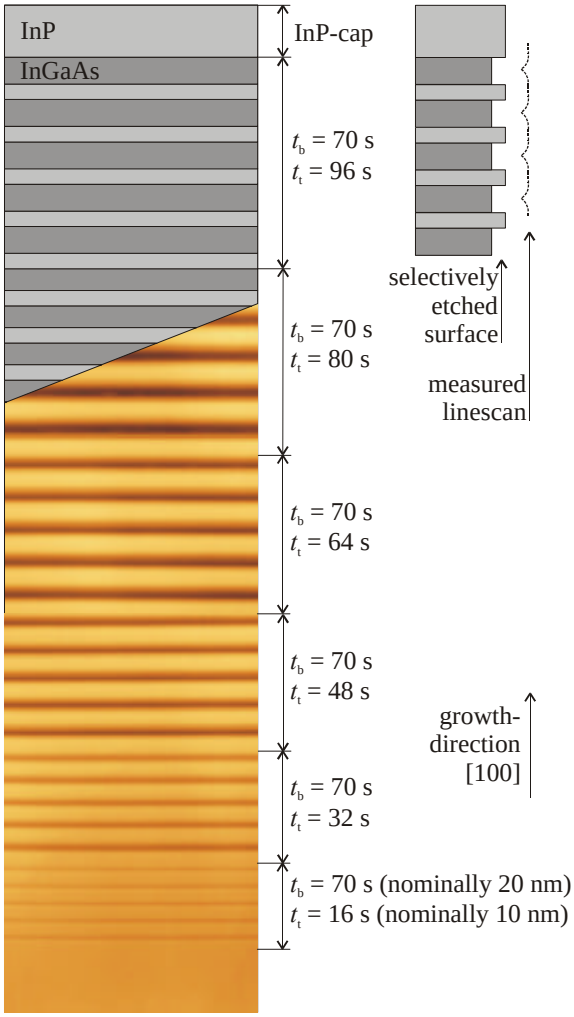

Fig. 1: AFM image of Sample 1. Measurement technique is shown in the upper right corner as a sideview of selectively etched structure.

cantilevers were used with a normal elastic constant of 0.032 Nm^{-1} and with specified radius of curvature of the probe tip of less then 50 nm with a scatter of ±15 nm. The AFM was especially calibrated to eliminate systematic errors like Abbe error or tube scanner nonlinearities [2]. To eliminate the influence of the probe-tip geometry, only the periodicity of the structures was considered, which is given by the lateral distance of two consecutive minima (e.g. periods 1 to 4 in Fig. 2). This was done by evaluating the derivative of each linescan [2]. One period corresponds to one double-layer thickness. The comparison of periods taken at different

locations and their statistical distribution reveals the homogeneity of the grown structure.

4. Homogeneity

The upper part of Fig. 2 represents a typical topograph measured and corrected as described in [2]. We want to arrive at significant results by evaluating only a few linescanes. This procedure is justified by a comparison of the 20 neighbouring linescans marked by the vertical bar L. Table 1 gives the means and deviations for the periods 1 to 4 within section L. The very small deviations clearly demonstrate that just one linescan is representative for a wide range. Evaluating consecutive periods with nominally identical thickness testifies its homogeneity. The four linescans a to d displayed in the lower part of Fig. 2 were evaluated and the results are given in Fig. 3. The standard deviations marked as error bars are always below one nanometer. Further cross-sections in different places of the whole sample were examined with similar results. For example the means of 4 consecutive periods of the double layers with 16 s growth duration of the InGaAs taken from different locations (Sample 1) are given in Table 2. The standard deviations are just as small as the ones shown in Table 1. Thus an excellent homogeneity is observed both in lateral and in growth direction, respectively. This proves that we have to measure only one linescan for reliable information.

Table 1: Evaluation of 20 linescans within section L (cf. Fig. 1).

period	mean (nm)	standard deviation (nm)
1	66.73	0.12
2	66.76	0.08
3	66.39	0.09
4	66.28	0.40

Table 2: Means of 4 periods evaluated from different locations (Sample 1).

period	mean (nm)	standard deviation (nm)
1	35.92	0.19
2	36.00	0.14
3	35.89	0.16
4	36.38	0.22

5. Growth Rates

The thickness D of a double-layer is given by the formula

$$D(t_t, t_b) = r_t\, t_t + r_b\, t_b, \quad (1)$$

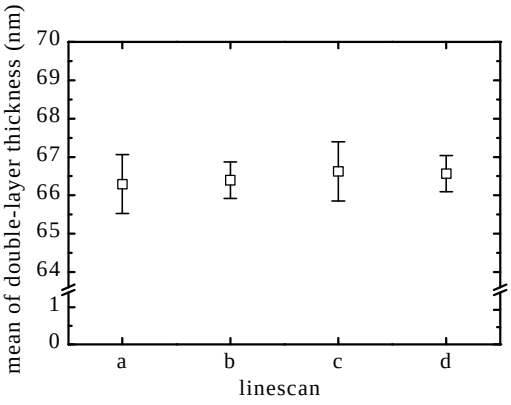

Fig. 3: Mean value of double-layer along the linescans a to d (cf. Fig. 1).

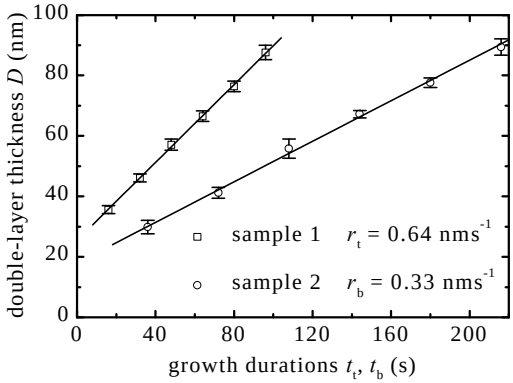

Fig. 4: Double-layer thickness D versus growth durations t_t and t_b of the ternary layer and the binary layer, respectively.

where r_b is the growth rate of InP. The growth rate r_t of the ternary layer can be obtained from the slope of D if t_b remained constant. This was done in the case of Sample 1. The measured values $D(t_t)$, all taken for t_b = 70 s, are plotted versus the InGaAs-growth duration t_t in Fig. 4 (open squares). The bars indicate the statistical error of standard deviation and the error left after calibration of the AFM [2]. We find $r_t = 0.64\ \mathrm{nms}^{-1}$ from the slope of $D(t_t)$. The growth rate of InP r_b was evaluated from Sample 2, where the ternary layer thickness remained constant and the binary one was varied. The measured double-layer thicknesses are displayed in Fig. 4 as open cycles. We find just as described above for the binary layer growth rate $r_b = 0.33\ \mathrm{nms}^{-1}$. We note for further investigations into epitaxial growth that the growth rate of InP is about one half of the ternary growth rate.

6. Conclusion

In conclusion we have developed an efficient tool to determine the homogeneity of nanostructures for materials engineering of MOVPE growth. In addition we determine precisely the growth rate of epitaxial layers for advanced quantum devices down to the nanometer scale.

Acknowledgement

This work was generously supported by the Volkswagen-Stiftung and the Deutsche Forschungsgemeinschaft.

References

[1] H. Chen, R. M. Feenstra, R. S. Goldman, C. Silfvenius, G. Landgren, *Appl. Phys. Lett.* **72** (14), 1727-1729, 1998.

[2] D. Wüllner, A. Schlachetzki, P. Bönsch, H.-H. Wehmann, T. Schrimpf, R. Lacmann, S. Kipp, *Mater. Sci. Eng.* **B51**, 178-187, 1998.

[3] A. V. Ankudinov, A. N. Titkov, T. V. Shubina, S. V. Ivanov, P. S. Kop'ev, H.-J. Lugauer, G. Reuscher, M. Keim, A. Waag, G. Landwehr, *Appl. Phys. Lett.* **75** (17), 2626-2628, 1999.

[4] P. A. Rosenthal, E. T. Yu, R. L. Pierson, P. J. Zampardi, *J. Appl. Phys.* **87** (4), 1937-1942, 2000.

[5] H. Hardtdegen, M. Hollfelder, C. Ungermanns, T. Raafat, R. Carius, A. Förster, J. Lange, H. Lüth, *Inst. Phys. Conf. Ser.* **141**, 81-86, 1995.

[6] S. R. Kurtz, A. A. Allermann, R. M. Biefeld, K. C. Baucom, *Appl. Phys. Lett.* **72** (17), 2093-2095, 1998.

[7] H.-H. Wehmann, A. Schlachetzki, in *Proceedings of the ESSDERC'89 Conference*, A. Heuberger, H. Ryssel, P. Lange, Eds., Berlin: Springer, Germany, 1989, pp. 491-494.